Statistical Modelling for Prediction of CCT Diagrams of Steels Involving Interaction of Alloying Elements

Henry Martin[a,b,*], Peter Amoako-Yirenkyi[a,c], Aarne Pohjonen[d], Nana K. Frempong[a,e], Jukka Komi[d], Mahesh Somani[d]

[a] *Center for Scientific and Technical Computing, National Institute for Mathematical Sciences, Kumasi, Ghana*
[b] *Department of Physics, Kwame Nkrumah University of Science and Technology, Kumasi, Ghana*
[c] *Department of Mathematics, Kwame Nkrumah University of Science and Technology, Kumasi, Ghana*
[d] *Materials and Production Technology, University of Oulu, Pentti Kaiteran katu 1, 90014 Oulu, Finland*
[e] *Department of Statistics, Kwame Nkrumah University of Science and Technology, Kumasi, Ghana*

Abstract

The interaction of different alloying elements has a significant impact on the mechanical and microstructural properties of steel products due to the thermodynamic and kinetic effect. This paper presents a statistically developed and validated model for austenite decomposition during cooling based on a set of experimental Continuous Cooling Transformation (CCT) diagrams available in literature. In the model, two-way interactions of the alloying elements are included as add-on terms and the procedure for the analysis ensures there is no overfitting. The model can be used to predict phase transformation temperatures and critical cooling rates for the formation of polygonal ferrite, bainite or martensite for the production of steel.

Keywords: `Modelling`, 2-way interaction, CCT diagrams, Longitudinal data, Stepwise regression, Influential diagnostic, Austenite decomposition, Steel

*Henry Martin
Email address: `hmartin@nims.edu.gh / hmartin@knust.edu.gh` (Henry Martin)

1. Introduction

Steel is used in a wide variety of applications, which require specific mechanical properties. In order to achieve the desired properties, thermomechanical processing techniques are used, followed by continuous cooling that results in specific microstructural evolution through phase transformation. This naturally influences the combined requisite property. During the processing, materials can be either deformed in austenitic state (or as-cast from melt) and then cooled to room temperature. In the cooling stage, austenite can decompose to ferrite phase types roughly classified as (polygonal) ferrite, bainite and martensite. Since the different ferritic phases have decisive influence on the mechanical properties, it is important to control the austenite decomposition process. The most important factor affecting the austenite decomposition is the chemical composition of the steel and the applied cooling path.

The austenite decomposition is conventionally represented using time-temperature diagrams, either for holding at constant temperature (TTT, Time Temperature Transformation diagrams) or for cooling at different rates (CCT, Continuous Cooling Transformation diagrams). The TTT diagram can be used to calculate an estimate for the transformation start using the Scheil's additivity rule[37, 40], but since there is a considerable difference in the long time isothermal holding and fast continuous cooling, the usage of CCT diagram gives better estimate for the transformation onset during rapid cooling. Since fast cooling rates are often used in steel production, predicting the decomposition of austenite using CCT diagrams has been the subject of several earlier studies[41, 36, 18]. Earlier studies by reference [31], [33] and [19] focused on the usage of an additive regression model of chemical composition as well as the cooling path effect for the start of transformation of ferrite, bainite and martensite respectively. In these earlier studies, the interaction of different alloying elements was not taken into account, instead the applied model assumed linear dependence of alloying elements. Unfortunately, the physical interpretation of the overall transformation kinetic of undercooled austenite in steel is determined by several factors, such

as the mobility of the compositional atoms participating in the transformation. This results in solute microsegregation, formation of precipitates, etc which signifies interaction among the alloying elements. Therefore using additive model does not practically represent the physical phenomenon.

In order to address this challenge, we present in this paper a model that takes into account the interaction as well as the quadratic dependence of alloying elements on the transformation onset. This provides better description of the experimental data since only the most significant interaction and quadratic alloying element terms were considered. This enables all the individual alloying elements to be significant to the time dependent growth and the response temperature. The efficiency of the current model has been further examined by fitting it with the CCT behavior of several steels, represented in [44, 9] which focuses on molybdenum containing steels.

2. Methodology and Model Formulation

This paper is intended to develop a methodology in order to model, analyze and validate the characteristic curves for the onset of autensite decomposition into the three main primary undercooled phases, polygonal ferrite, bainite and martensite, which are normally present on the CCT diagrams. A range of molybdenum-containing steels with a widely varied compositions and different combinations of alloying elements (2-ways of interaction) were used in fitting a linear model. The construction of a longitudinal data (i.e an unbalanced time variation experimental data points)[24] in the field of statistical modelling and analysis was employed[10, 16, 4, 38]. The transformation start curves marking austenite decomposition were extracted from various CCT diagrams in literature[44, 9], thus encompassing 68 curves of ferrite formation, 52 curves of bainite formation and 26 curves of martensite formation as shown in Fig. 1.

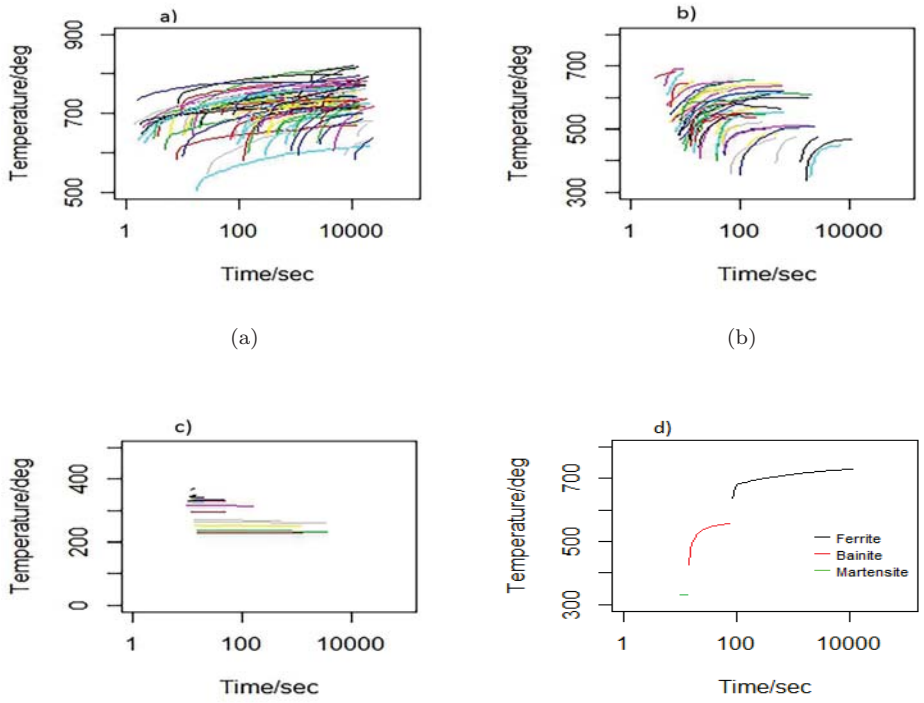

(a) (b)

(c) (d)

Figure 1: Extracted experimental austenite decomposition start curves from various continuous cooling transformation (CCT) diagrams with a) depicting 68 ferrite start curves, b) depicting 52 bainite start curves, c) depicting 26 martensite start curves and d) corresponding curves for single steel grade of 0.39% C - 0.82% Mn - 0.26% Si - 0.21% Mo - 1.0% Cr.

The chemical compositions shown in Table 1, gives the range of mass concentration (in wt. %) of alloying elements used in this study.

Table 1: Range of mass concentration (wt. %) of elements

Ferrite Onset Formation								
Range	C	Mn	Si	Mo	Ni	Cr	B	Co
min	0.097	0.32	0.16	0	0	0	0	0
max	0.41	1.47	1.5	0.95	4.45	3.76	0.006	3.9
Bainite Onset Formation								
min	0.097	0.32	0.16	0	0	0	0	0
max	0.41	1.47	1.5	0.95	4.43	1.54	0.006	3.9
Martensite Onset Formation								
min	0.3	0.68	0.26	0.21	0	0	0	0
max	0.41	1.45	1.5	0.82	4.43	1.54	0	0

2.1. Model Formulation

In the current study, our intention is to develop a statistical model, analyse and validate the dataset describing large number of CCT diagrams. An example of such diagram for one steel is shown in Fig. 1d. The construction of statistically based models for phase transformation is not new as researchers in this field seek to simulate the behavior by drawing a relationship between the fractional weight of alloying elements, (c), the temperature, (T), and the time required for the undercooled formation of phases, (t). The alloying elements play a very crucial role in the transformation and in recent times it has become even more important to understand, ascertain and interpret their interaction that would provide a better understanding concerning various microstructural phenomena, such as precipitation, microsegregation and other physical phenomena that happens in the thermomechanical processing. The current article describes in detail the statistical models that were fitted to the experimental data and the approach that provided the best fit to the data.

2.1.1. Additive Regression Model

For both polygonal ferrite and bainite we first fitted the time coordinate (t_{cr}) corresponding to the fastest cooling rate that produces the given phase, and then we fitted the coefficients α which describe the effect of alloying on the transformation temperature while β is the intercept for the response temperature and δ is the amplitude for the inverse hyperbolic sine function. The different model formulations are given below. The implementation of Equation (AS 1 and AS 2) represents the relation of additive function of alloying elements and time dependent growth of ferrite and bainite at a given response temperature. Equation AS 2 is a newly proposed model that contains a function to decrease the slope steepness for the onset of ferrite and bainite as compared to the existing model of Equation AS 1[31, 32]. On the other hand, Equation AS 3 concerns the formation of martensite[45, 19], thus presenting time independent growth since its response temperature is constant. Finally, Equation AS 4 depicts logarithmic time for critical cooling rate in relation to the additive function of alloying elements that takes care of any form of skewness in Equation (AS 1 and AS 2).

$$T = \beta + \sum_{l}^{k} \alpha_l c_l + \delta \operatorname{arcsinh}(t - t_{cr}) + \epsilon \tag{AS 1}$$

$$T = \beta + \sum_{l}^{k} \alpha_l c_l + \delta \operatorname{arcsinh}(\log_{10}(1 + t - t_{cr})) + \epsilon \tag{AS 2}$$

$$T = \beta + \sum_{l}^{k} \alpha_l c_l + \epsilon \tag{AS 3}$$

$$\log_{10} t_{cr} = \beta + \sum_{l}^{k} \alpha_l c_l + \epsilon \tag{AS 4}$$

2.1.2. Interaction of Alloying Elements

Alloying elements may have different interacting effects, either individually or in combination, both from a thermodynamic and kinetic point of view. Thermodynamics affects the driving force for the transformations and grain boundary segregation, and the speed of the transformation is affected by the atomic mobilities, which are also subjected to interactions. The Grossman formulation of

hardenability used as todays' bench-mark is based on all kinds of interaction terms[14].

The atoms react with each other in any composition affecting the microstructural processes, such as nucleation, micro-segregation and precipitation in steel processing. Hence, it is prudent that, terms defining interaction of elements are included in the additive regression model. In statistical modelling this is formulated as follows: when the effect of a predictor on the response depends on another predictor[2, 3, 15, 27] or an interaction of a predictor variable with itself. The former is sometimes referred to as a multiplicative interaction[8, 7] and the latter a quadratic effect.

These additional terms have been ignored in most earlier models for the onset of phase formation in phase transformation of steel except for modelling C-Mn steel[39, 11]. Both the interaction of two different alloying elements as well as the quadratic effect of all individual alloying elements were employed for bainite formation. Also the quadratic effect of individual alloying elements was assessed in connection with martensite transformation in medium carbon S355 steel covering both the modelling of start temperature as well as the prediction of mechanical properties[29, 46].

A 2-way interaction, which incorporates either a single combination of two alloying elements or a quadratic effect of a single alloying element or both is added to the model in Equation (AS 1 - AS 4) to obtain the interaction model shown in Equation (I 1 - I 4). This is done using a stepwise regression method[13, 17] to finalize a model that shows a reasonable effect, thus comprising good fitting using the model and the significance of all the individual alloying elements and their interaction in relation to the response temperature and time dependent growth[24].

$$T = \beta + \sum_{l}^{k} \alpha_l c_l + \delta \operatorname{arcsinh}(t - t_{cr}) + \sum_{\substack{l,j \\ \langle l<j \rangle}}^{2} A_{lj} c_l c_j + \epsilon \qquad \text{(I 1)}$$

$$T = \beta + \sum_{l}^{k} \alpha_l c_l + \delta \operatorname{arcsinh}(\log_{10}(1 + t - t_{cr})) + \sum_{\substack{l,j \\ \langle l<j \rangle}}^{2} A_{lj} c_l c_j + \epsilon \qquad \text{(I 2)}$$

$$T = \beta + \sum_{l}^{k} \alpha_l c_l + \sum_{\substack{l,j \\ <l=j>}}^{2} B_{lj} c_l c_j + \epsilon \qquad \text{(I 3)}$$

$$\log_{10} t_{cr} = \beta + \sum_{l}^{k} \alpha_l c_l + \sum_{\substack{l,j \\ <l=j>}}^{2} B_{lj} c_l c_j + \sum_{\substack{l,j \\ \langle l<j \rangle}}^{2} A_{lj} c_l c_j + \epsilon \qquad \text{(I 4)}$$

3. Results and Discussion

The influence of combining alloy elements (i.e. 2-way interaction) to reveal the impact of alloying elements on existing phase transformation model (additive regression) describing the decomposition of austenite in steel, was modelled, and analyzed as described in the previous section using mathematical and computational modelling and simulation tools (SAS[35], R and MATLAB) and statistical validation was conducted, as explained in section 3.2.

Table 2 shows the goodness of fit statistics for the additive model (Eqn. AS 1 - AS 3) and the best alloying elements interaction attained for the new model (Eqn. I 1 - I 3).

Table 2: Criteria (fit statistics) for additive and interaction models for polygonal ferrite, bainite and martensite

Onset of Ferrite Formation				
Models	-2ℓ	AIC	AICC	BIC
AS 1	10122.2	10146.2	10146.5	10172.3
AS 2	10256.9	10280.9	10281.2	10307.0
I 1	10105.3	10131.3	10131.6	10159.6
I 2	10239.1	10265.1	10265.4	10293.4
Onset of Bainite Formation				
AS 1	8489.6	8513.6	8513.9	8536.6
AS 2	8353.1	8377.1	8377.4	8400.0
I 1	8477.6	8505.6	8506.0	8532.4
I 2	8342.1	8370.1	8370.5	8396.9
Onset of Martensite Formation				
AS 3	10687.4	10711.4	10711.7	10738.1
I 3	10239.1	10265.1	10265.4	10293.4

From the statistics presented in Table (2), the different selection criteria shows how extensive (or little) information is lost for a model to obtain its observed data (thus the smaller the value the better the fit). This, in effect shows the quality of a model that is able to replicate the observed data, hence causing relatively less error in prediction. Four types of criteria (thus, -2ℓ, AIC, AICC and BIC) are used in this study mainly to show that an add-on of terms to the additive model (Eqn. AS 1 -AS 4) is not causing any overfitting of parameter estimate[24]. The goodness of fit measurement shown in Table 2 depict the criteria for all of the models displayed from the table. This indicates that the addition of an interaction term (thus combining alloying elements) gives the best fitness (i.e. the best model described by Eqn. (I 1 - I 4) and the parameters given in Tables 4, 6, 8 and 10).

Also, it is clear from Figure 2 - 4 that the data set with removed sample id's has a very good fitness measure. A global sensitivity analysis on studying the variation between steel grades (Influence diagnostics) was conducted on the additive model (Eqn. AS 1 - AS 3) employing the Cook's Distance (D_i) statistics for influence parameter estimate and CovRatio for the influence precision[24].

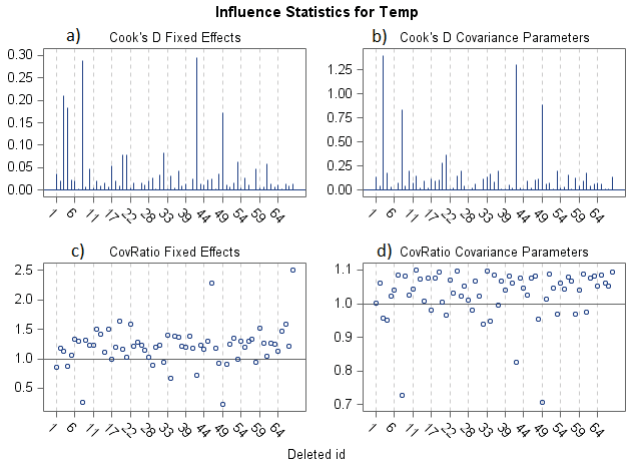

Figure 2: Ferrite formation influence diagnostics of steel grades measuring a) Cook's D fixed effects, b) Cook's D covariance parameters, c) CovRatio fixed effects, d) CovRatio covariance parameters

Having known the influence of each steel grade on the parameter estimates for the additive model, a suitable decision was taken to delete any sample which did not give any positive contribution to the extension/adaptability of the model for any steel composition with the range shown in Table 1.

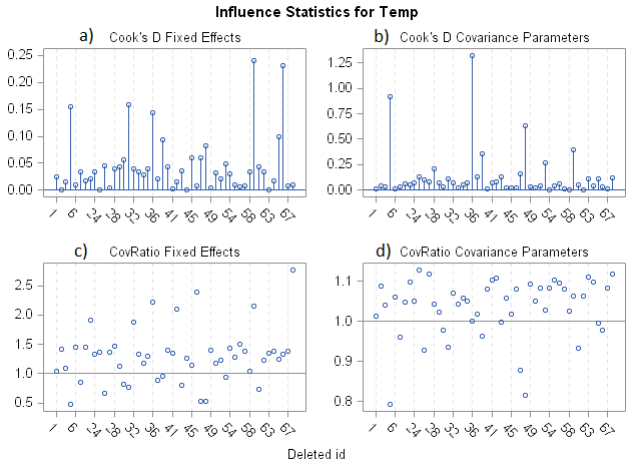

Figure 3: Bainite formation influence diagnostics of steel grades measuring a) Cook's D fixed effects, b) Cook's D covariance parameters, c) CovRatio fixed effects, d) CovRatio covariance parameters

Figure 2 - 4 shows the manner in which almost all the samples are at least contributing to the influence of parameter estimate even though only few of them have relatively higher impact than others (thus D values > 0.2), which is less than a very influential sample as known by a cutoff value of 1. Also very few samples has a degradable precision which do not affect the estimates badly given that their impact is not that of a threat to the estimates. Therefore, the full data set with some sample ids with much more degradable precision can be removed for a good dataset to generate a usable, adaptable and extendable model with other steel composition within the range provided.

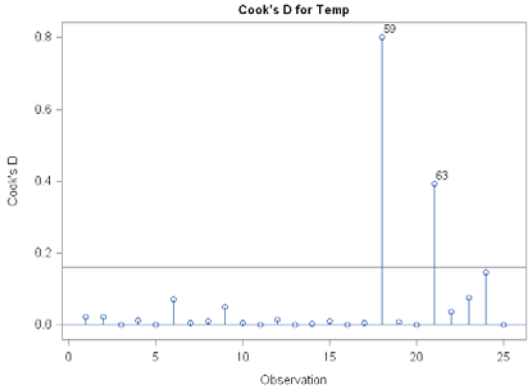

Figure 4: Martensite formation influence diagnostics of steel grades

We continue with testing the significance (thus $Pr < 0.05$) of the alloying elements and their interaction while checking the goodness of fits statistics (thus, -2ℓ, AIC, AICC and BIC) for each model (Eqn. AS 1 - I 4). This numerical test comparison ascertain the combined alloying element (interaction) that affects the selected additive model positively. This was done chronologically for all the phases. For example, for the formation of polygonal ferrite, Table 3 and 4 indicates the significance for all the individual elements and its interaction in the models (thus additive model (Eqn. AS 1 and AS 2) and interaction model (Eqn. I 1 and I 2) when the set of three sample ids were removed from the initial dataset of ferrite formation). Again, this shows that the best fit is the interaction of alloying elements model (Eqn. I 1) because apart from the interaction (C*Ni) itself showing high significance value, it also changed the individual elements (thus those marked red) to be also significant(thus those marked blue).

Ferrite

Table 3: Parameter estimates for the polygonal ferrite additive model

AS 1				AS 2			
Effect		Estimate	Pr $> \|t\|$	Effect		Estimate	Pr $> \|t\|$
Intercept	β	773.59	$< .0001$	Intercept	β	761.27	$< .0001$
C	α_l	-160.92	$< .0001$	C	α_l	-152.07	$< .0001$
Mn		-63.2933	$< .0001$	Mn		-62.6536	$< .0001$
Si		16.1381	0.0047	Si		16.3829	0.0049
Ni		-32.1110	$< .0001$	Ni		-31.5361	$< .0001$
Mo		-19.5573	0.0078	Mo		-19.0940	0.0108
Cr		-13.5218	0.0023	Cr		-13.5748	0.0027
B		-2010.97	**0.2373**	**B**		-1454.33	**0.4014**
Co		6.0766	**0.0679**	**Co**		5.8853	**0.0831**
δ		9.5706	$< .0001$	δ		44.4968	$< .0001$

Table 4: Parameter estimates for the polygonal ferrite interaction model

I 1				I 2			
Effect		Estimate	Pr > |t|	Effect		Estimate	Pr > |t|
Intercept	β	796.97	< .0001	Intercept	β	785.75	< .0001
C		-243.37	< .0001	C		-238.33	< .0001
Mn		-55.5699	< .0001	Mn		-54.5785	< .0001
Si		18.4717	0.0003	Si		18.8225	0.0003
Ni	α_l	-53.9073	< .0001	Ni	α_l	-54.3365	< .0001
Mo		-22.7219	0.0006	Mo		-22.4077	0.0009
Cr		-15.3014	0.0001	Cr		-15.4388	0.0002
B		-4182.67	**0.0095**	**B**		-3727.63	**0.0218**
Co		8.3326	**0.0059**	**Co**		8.2448	**0.0071**
C*Ni	A_{lj}	63.0462	< .0001	**C*Ni**	A_{lj}	65.9392	< .0001
δ		9.5621	< .0001	δ		44.4567	< .0001

In addition to undertaking the above numerical test comparison for all phases in this paper, we further conducted an influential diagnostic test on the observation location space for fastest cooling rate (t_{cr}) of ferrite and bainite in Equation AS 4 and I 4 and the martensite onset temperature in Equation AS 3 and I 3. Location of observations plays an important role in the estimation of predicted values, regression estimates and other model summary statistics such as the adjusted R^2 and Root Mean Square Error (RMSE) for an add-on parameter (thus the interaction). These are shown in Tables (5, 9 and 11) for ferrite, bainite and martensite respectively, supporting the argument in Tables (6, 10 and 12) that the interaction of the alloying element yields better goodness of fit for the time of critical cooling rate of ferrite and bainite as well as for the martensite onset temperature. As shown, Equation (I 4) has less error as compared to additive regression Equation (AS 4). Also, the variation from the predicted value (thus Adj R^2) gets closer to 1 than in the case of the additive regression equation showing the extensiveness of an add-on interaction terms fits the data well.

These influential diagnostic test (thus predicted value, outlier and leverage) on the observation location space are shown on Figures (5 and 6), (7 and 8) and (9 and 10) for polygonal ferrite, bainite and martensite respectively.

Table 5: Onset of ferrite model fit statistics for time of critical cooling rate

Model	R^2	Adj R^2	RMSE
AS 4	0.8054	0.7776	0.52844
I 4	0.9265	0.9095	0.33705

Table 6: Parameter estimates of the time for the critical cooling rate models for ferrite onset

AS 4				I 4			
Effect		Estimate	Pr $>\|t\|$	Effect		Estimate	Pr $>\|t\|$
Intercept	β	-1.5962	0.0034	Intercept	β	-2.2898	$<$ .0001
C		2.5496	0.0275	C		3.0372	0.0002
Mn		1.15167	0.0037	Mn		1.5427	$<$ .0001
Si		0.0102	**0.9601**	**Si**		0.06265	**0.6332**
Ni		0.4597	$<$ .0001	Ni		0.2723	$<$ .0001
Mo	α_l	3.2113	$<$ .0001	Mo	α_l	6.5357	$<$ .0001
Cr		0.5868	0.0004	Cr		0.4426	0.0002
B		320.62	$<$ .0001	B		827.7659	$<$ .0001
Co		-0.1705	**0.1665**	**Co**		-11.69184	**0.0418**
-	B_{ij}	-	-	**Mo*Mo**	B_{lj}	-4.90195	$<$ .0001
-		-	-	**B*B**		-89309	**0.0045**
-	A_{lj}	-	-	**Mo*Ni**	A_{lj}	0.6626	**0.0011**
-		-	-	**C*Co**		29.6718	**0.0416**

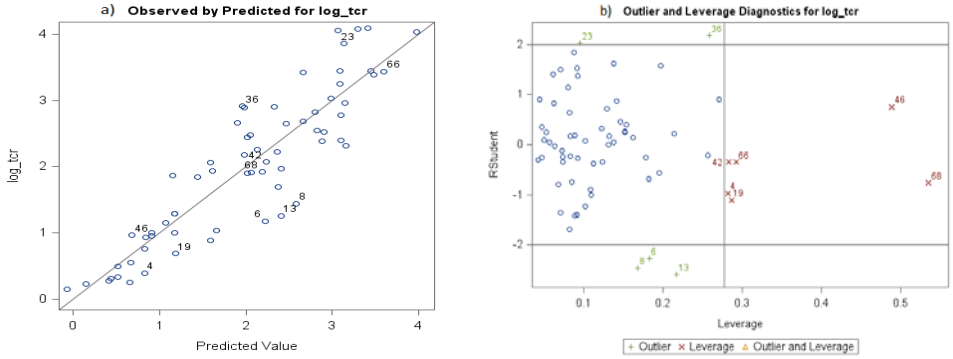

(a) (b)

Figure 5: Ferrite onset time of critical cooling rate for additive model indicating a) comparison of predicted fit to data and b) outlier and leverage diagnostics

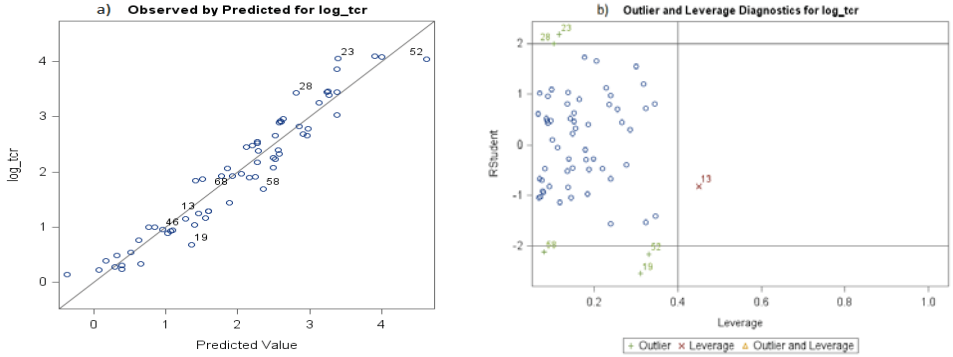

(a) (b)

Figure 6: Ferrite onset time of critical cooling rate for interaction model indicating a) comparison of predicted fit to data and b) outlier and leverage diagnostics

Bainite

Table 7: Parameter estimates for the onset bainite additive model

AS 1				AS 2			
Effect		Estimate	Pr $> \|t\|$	Effect		Estimate	Pr $> \|t\|$
Intercept	β	899.61	$< .0001$	Intercept	β	886.50	$< .0001$
C		-551.68	$< .0001$	C		-539.14	$< .0001$
Mn		-102.83	$< .0001$	Mn		-102.27	$< .0001$
Si		-6.7191	**0.5461**	**Si**		-6.2975	**0.5650**
Ni	α_l	-60.2258	$< .0001$	Ni	α_l	-58.3767	$< .0001$
Mo		-183.14	$< .0001$	Mo		-183.64	$< .0001$
Cr		-89.9940	$< .0001$	Cr		-90.9165	$< .0001$
B		-24458	$< .0001$	B		-23816	$< .0001$
Co		25.6220	$< .0001$	Co		25.8393	$< .0001$
δ		18.8214	$< .0001$	δ		74.8521	$< .0001$

Table 8: Parameter estimates for the onset bainite interaction model

I 1				I 2			
Effect		Estimate	Pr > |t|	Effect		Estimate	Pr > |t|
Intercept	β	871.93	< .0001	Intercept	β	859.24	< .0001
C		-572.32	< .0001	C		-559.36	< .0001
Mn		-97.5479	< .0001	Mn		-96.4405	< .0001
Si		44.3756	**0.0507**	**Si**		43.5439	**0.0537**
Ni	α_l	-46.6330	< .0001	Ni	α_l	-45.9549	< .0001
Mo		-117.56	< .0001	Mo		-120.91	< .0001
Cr		-86.8119	< .0001	Cr		-87.8734	< .0001
B		-25252	< .0001	B		-24516	< .0001
Co		23.0973	0.0001	Co		23.6204	< .0001
Si*Mo	A_{lj}	-102.70	**0.0084**	**Si*Mo**	A_{lj}	-99.7102	**0.0100**
Ni*Mo		-43.1331	**0.0114**	**Ni*Mo**		-39.0975	**0.0202**
δ		18.8267	< .0001	δ		74.8666	< .0001

Table 9: Onset of bainite model fit statistics for time of critical cooling rate

Model	R^2	Adj R^2	RMSE
AS 4	0.8229	0.7884	0.34108
I 4	0.9434	0.9251	0.20299

Table 10: Parameter estimates of the time for the critical cooling rate models for bainite onset

AS 4				I 4			
Effect		Estimate	Pr > |t|	Effect		Estimate	Pr > |t|
Intercept	β	-1.3302	0.0032	Intercept	β	-8.19007	0.0029
C		4.6781	< .0001	C		20.4879	0.0039
Mn		0.2414	**0.4600**	**Mn**		7.28762	**0.0214**
Si		0.14070	**0.3939**	**Si**		0.30940	**0.0036**
Ni	α_l	0.5196	< .0001	Ni	α_l	0.66200	< .0001
Mo		0.8394	0.0017	Mo		1.16926	< .0001
Cr		0.4880	0.0002	Cr		0.73920	< .0001
B		150.2221	0.0025	B		2418.1819	< .0001
Co		-0.17431	**0.0534**	**Co**		-0.10468	**0.0646**
-	B_{lj}	-	-	**B*B**	B_{lj}	-157312	< .0001
-		-	-	**Ni*B**		-70.8405	< .0001
-	A_{lj}	-	-	**Mn*B**	A_{lj}	-1650.1143	**0.0038**
-		-	-	**C*Mn**		-17.1969	**0.0345**

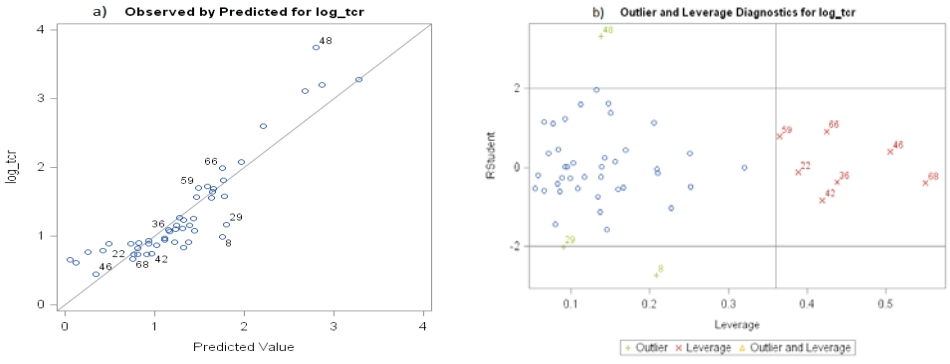

(a) (b)

Figure 7: Bainite onset time of critical cooling rate for additive model indicating a) comparison of predicted fit to data and b) outlier and leverage diagnostics

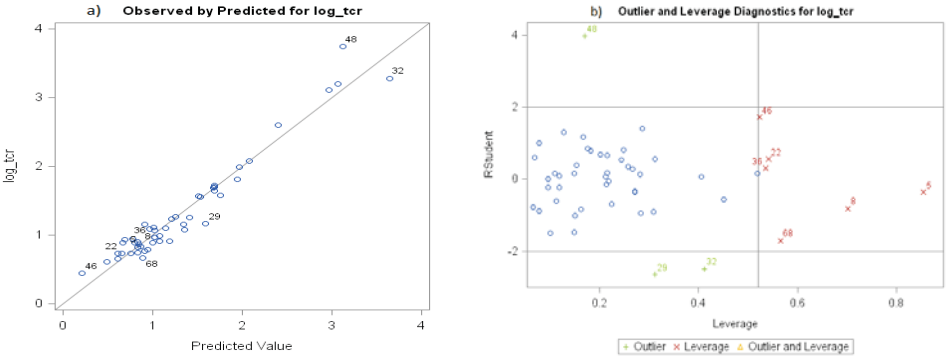

(a) (b)

Figure 8: Bainite onset time of critical cooling rate for interaction model indicating a) comparison of predicted fit to data and b) outlier and leverage diagnostics

Martensite

Table 11: Onset of martensite model AS 3 fit statistics for temperature

Model	R^2	Adj R^2	RMSE
AS 3	0.9022	0.8696	16.40373
I 3	0.9238	0.8925	14.89245

Table 12: Parameter estimates for the onset martensite additive and interaction models

AS 3				I 3			
Effect		Estimate	Pr > |t|	Effect		Estimate	Pr > |t|
Intercept	β	624.7086	< .0001	Intercept	β	406.6550	0.0015
C	α_l	-671.3039	< .0001	C	α_l	-843.1093	< .0001
Mn		-22.2523	**0.3219**	**Mn**		528.0025	**0.0506**
Si		-20.1481	**0.0711**	**Si**		-20.5010	**0.0463**
Ni		-25.4520	< .0001	Ni		-20.79077	< .0001
Mo		14.44503	**0.5745**	**Mo**		20.55019	**0.3860**
Cr		-17.6135	**0.1008**	**Cr**		-19.50909	**0.0508**
-	B_{lj}	-	-	**Mn*Mn**	B_{lj}	-250.93470	**0.0420**

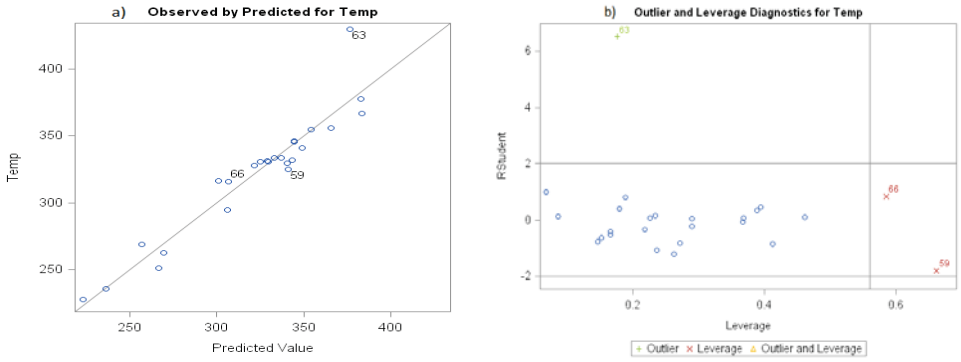

(a) (b)

Figure 9: Martensite temperature of onset for additive model indicating a) comparison of predicted fit to data and b) outlier and leverage diagnostics

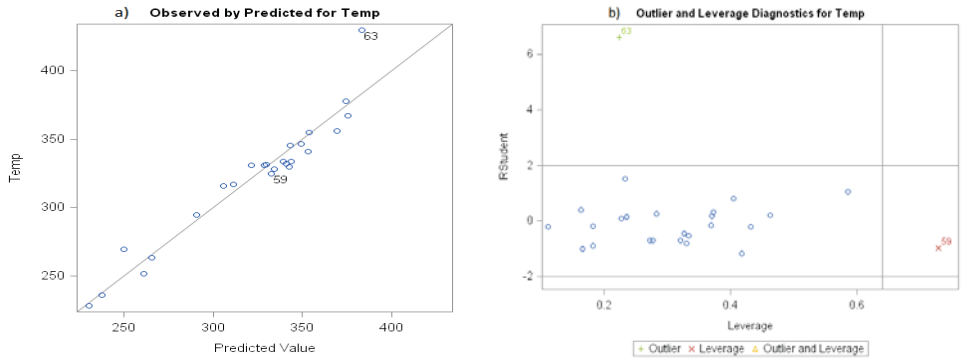

(a) (b)

Figure 10: Martensite temperature of onset for interaction model indicating a) comparison of predicted fit to data and b) outlier and leverage diagnostics

3.1. Discussion on the Interaction of Alloying Elements

The production of a new steel often requires heat treatment and a knowledge of the effect of alloying elements on the CCT diagram in order to achieve the desired final microstructure and mechanical properties[25]. Alloying elements affect the details of the CCT diagram through their effect on thermodynamic and kinetic parameters controlling the formation of ferrite, bainite and martensite[34, 5]. These are highly dependent on the type, amount and interaction of alloying elements. The alloying elements can be in solid solution or in precipitates and thereby affect the prior austenite grain size and condition of the austenite dislocation structure following any thermomechanical treatment[6]. Hence, they also affect the transformation start by changing the concentration of heterogeneous nucleation sites[31].

Alloying elements can be classified according to their chemical properties as carbide formers: Mn, Cr and Mo; non-carbide formers: Ni and Si; ferrite stabilizers: Mo and Si; and austenite stabilizers: Mn, C and Ni. Ref. [6] gives a qualitative description and physical explanation of all the single alloying element effects which agree with our results. C, Mn, Cr and Mo retard the phase transformation while Si promotes ferrite formation.

The nonlinearity relationship between the heat treatment and the alloying

elements is a known characteristic which specifies the interactions between the alloying elements[26]. This description was also confirmed in Ref. [43] with the occurrence of concave regions signifying the interaction between alloying elements of either enhancing or reducing each other's effects. This agrees with our results as Table 4 further shows the analysis of the interaction of C-Ni on ferrite transformation start with the physical contribution of high hardenability. The positive Ni*C term and high statistically significant value means that C depresses the start of the ferrite reaction less in the presence of Ni than otherwise. This interaction further acknowledges the hardenability modification of B and Co[22, 9] with also a statistically significant value. Table 6 continues with the time for the critical cooling rate. This again indicates the non-linearity with the interaction of C-Co, Mo-Ni, Mo^2 and B^2. All of these interactions obtained statistically significant values which caused Co to also be statistically significant. Mo^2 and B^2 indicates a way of balancing the hardenability of the steel. This has been explained with boron being the main factor of hardenability as it reduces the free energy of austenite grain boundaries due to segregation, retarding the nucleation of ferrite and bainite[42]. This result of interaction between Mo and Ni causes an increase in the delay of the start of ferrite transformation leading to the manifestation of hardenability. The presence of the interaction between C and Co introduces a faster austenite transformation which brings in a lower hardenability. Therefore, the C-Co interactions was a means of adjusting the hardenability contributed from Mo^2 interaction in the ferrite.

In the case of bainite onset parameters shown in Table 8 and 10, literature[12, 20, 1] confirms our results of interaction of alloying elements with several explanations: Nickel is known to reduce the critical cooling rates of bainite while silicon increases the critical cooling rate for ferrite and bainite. Hence, the report that the effect of molybdenum is enhanced by nickel[43]. Also, Mo exerts solute drag effect[28]. These are consistent with the analysis of our results indicating the Ni-Mo and Si-Mo interaction. This shows that the balance of reaction effect caused Si in Table 7 to be statistically significant in Table 8. Manganese being a weak carbide forming element and an austenite stabilizer, enhances the effect of

C by increasing carbon solubility in austenite. Therefore, the C-Mn interaction is understood to increase the incubation time for bainite transformation[21].

In the case of martensite temperature onset parameters, Mn^2 obtaining a statistically significant value causes Mn to also be significant in Table 12. It is of no doubt that manganese is known to also increase martensite hardenability due to its partitioning between the austenite and ferrite during transformation, inducing microsegregation and bands of course in hot rolled product[23]. Also, manganese is known to move the phase region of martensite to low temperature. The non-linearity effect of manganese from our results agrees with ref. [45, 43]. Finally, we think there is a need to have an analysis with an increased order of interaction to cater for the single insignificant value that was not achieved. An example is Si, Co and Mo in Table 6, 10 and 12 respectively.

3.2. Model Validation

Model validation is the task of confirming that the parameter estimates from the statistical model are acceptable by obtaining a response variable with less error using a data generating process. This process decides whether the numerical results quantifying hypothesized relationships between variables (i.e. significance of alloying elements and their interaction), obtained from regression analysis are acceptable as a descriptions of the data. This is based on the data that was used in the construction of the model which involves analyzing the goodness of fit of the model. We performed this test using 5 different sample ids with an in-house MATLAB code to generate Figures (11 - 15).

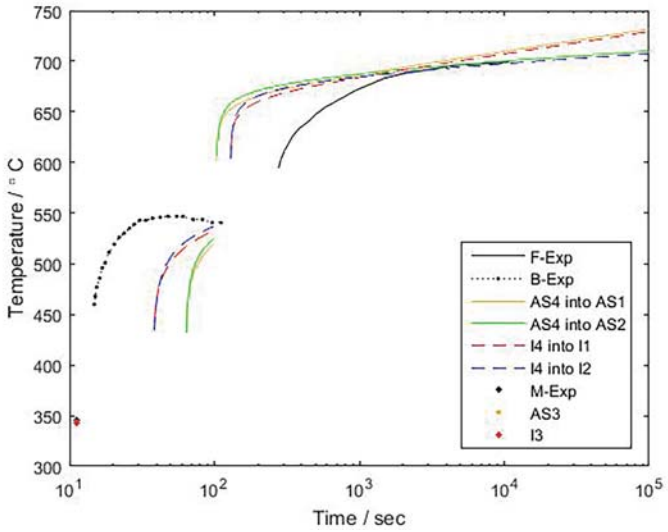

Figure 11: Model validation for Sample id 29 with composition (0.3% C - 0.69% Mn - 0.38% Si - 0.24% Mo - 1.79% Ni - 0.78% Cr)

The construction of the best model (interaction of alloying elements) can be attained by replacing the parameter estimates (i.e. α_l, β, δ, B_{lj} and A_{lj}) in Equations. (I 1 - I 4) with the value obtained by the statistical modelling and analysis given in Tables 4, 6, 8 and 10.

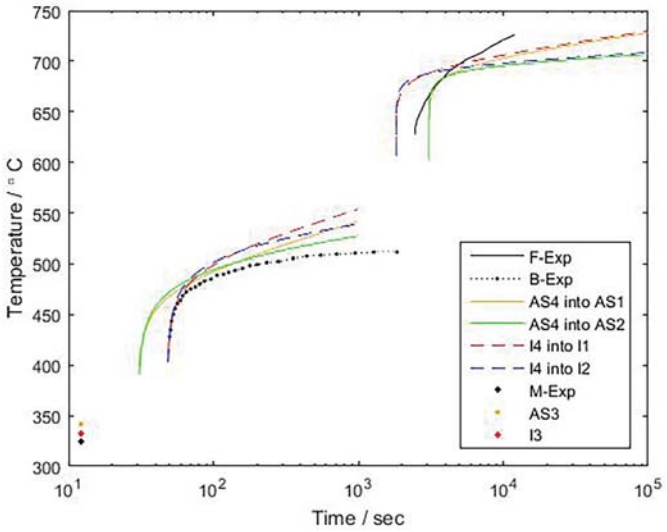

Figure 12: Model validation for Sample id 59 with composition (0.38% C - 1.45% Mn - 0.36% Si - 0.76% Mo)

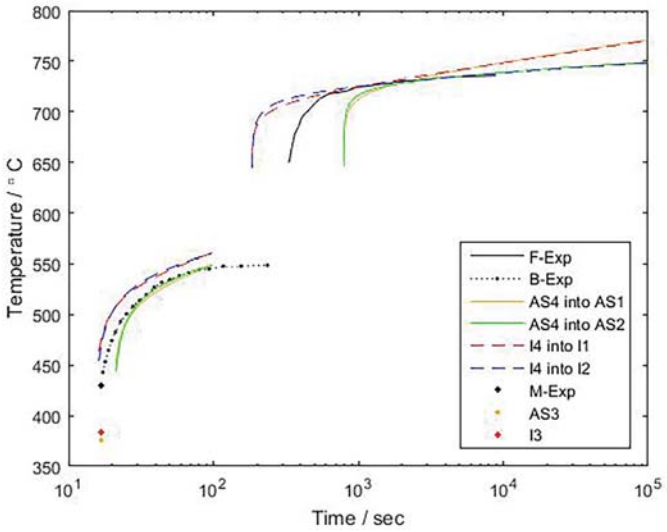

Figure 13: Model validation for Sample id 63 with composition (0.34% C - 0.8% Mn - 0.38% Si - 0.78% Mo - 0.34% Cr)

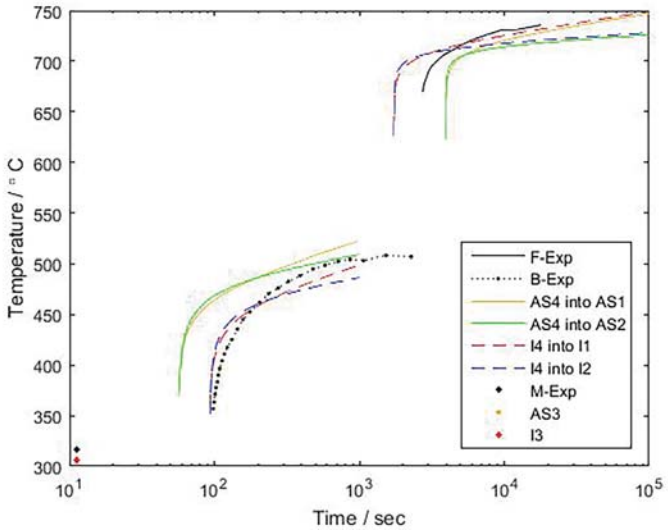

Figure 14: Model validation for Sample id 66 with composition (0.4% C - 1.38% Mn - 1.5% Si - 0.8% Mo)

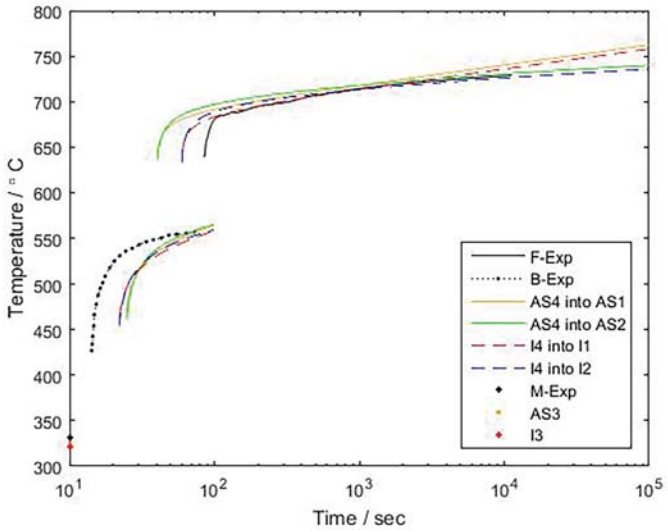

Figure 15: Model validation for Sample id 24 with composition (0.39% C - 0.82% Mn - 0.26% Si - 0.21% Mo - 1.0% Cr)

4. Conclusion

The combined effects of pairs of alloying elements (2-way interactions) in the prediction of CCT diagrams has been quantitatively modelled, analysed and validated. The approach used provides a novel way of constructing a model to predict austenitic decomposition for use in steel development. Unlike with previous models [11, 30, 31], this paper has shown that an add-on term improves the fit without causing overfitting. Finally, apart from the add-on terms (interaction of alloying elements i.e. 2-way or quadratic) itself showing high significance value ($Pr < .0001$), it also improved the significance of some of the individual elements and further totally caused others to be significant ($Pr < 0.05$) to the response temperature and critical cooling rate. We found that, out of the tested models, the best description for the CCT start curves are given by the following equations: The ferrite start curve $T_f(t)$ is described by Eqn.(1)

$$\begin{aligned} T_f(t) = {} & 796.97 - 243.37C - 55.70Mn + 18.47Si - 53.91Ni \\ & - 22.72Mo - 15.30Cr - 4182.67B + 8.33Co + 63.05CNi \\ & + 9.56 \operatorname{arcsinh}(t - t_{cr,f}) \end{aligned} \tag{1}$$

where $t \geq t_{cr,f}$. The critical cooling time for ferrite, $t_{cr,f}$, is obtained from Eqn.(2)

$$\begin{aligned} \log_{10}(t_{cr,f}) = {} & -2.29 + 3.04C + 1.54Mn + 0.063Si + 0.27Ni + 6.54Mo \\ & + 0.44Cr + 827.77B - 11.69Co - 4.90Mo^2 - 89309B^2 \\ & + 0.66MoNi + 29.67CCo \end{aligned} \tag{2}$$

The bainite start curve $T_b(t)$ is described by Eqn.(3)

$$\begin{aligned} T_b(t) = {} & 859.24 - 559.36C - 96.44Mn + 43.54Si - 45.95Ni - 120.91Mo \\ & - 87.87Cr - 24516B + 23.62Co - 99.71SiMo - 39.10NiMo \\ & + 74.87 \operatorname{arcsinh}(\log_{10}(1 + t - t_{cr,b})) \end{aligned} \tag{3}$$

where $t \geq t_{cr,b}$. The critical cooling time for bainite, $t_{cr,b}$, is obtained from

Eqn.(4)

$$\begin{aligned}\log_{10}(t_{cr,b}) = &-8.19 + 20.49C + 7.29Mn + 0.31Si + 0.66Ni \\ &+ 1.17Mo + 0.74Cr + 2418.18B - 0.10Co - 70.84NiB \\ &- 1650.11MnB - 17.20CMn - 157312B^2 \end{aligned} \tag{4}$$

and the martensite start temperature is given by Eqn.(5)

$$\begin{aligned}T_m = &\ 406.66 - 843.11C + 528.00Mn - 20.50Si - 20.79Ni \\ &+ 20.55Mo - 19.51Cr - 250.93Mn^2 \end{aligned} \tag{5}$$

where the alloying elements (C, Mn, Si, Ni, Mo, Cr, B, Co) are given in (wt. %).

5. Acknowledgements

Centre for Scientific and Technical Computing, National Institute for Mathematical Sciences hosted by Kwame Nkrumah University of Science and Technology Kumasi, Ghana. The University of Oulu under the research activity Genome of Steel project by the Academy of Finland. The authors would finally like to thank Prof. David Porter at University of Oulu, Materials and Production Technology, Oulu, Finland for his helpful discussion and insightful advice.

References

[1] H. Aaronson, W. Reynolds, G. Shiflet, and G. Spanos: *Metallurgical Transactions A*, 1990, vol. 21, pp. 1343–1380.

[2] P. D. Allison: *American Journal of Sociology*, 1977, vol. 83, pp. 144–153.

[3] H. O. Balli and B. E. Sørensen: *Empirical Economics*, 2013, vol. 45, pp. 583–603.

[4] P. B. Baltes and J. R. Nesselroade: *History and rational of longitudinal research. In Longitudinal Research in the Study of Behavior and Development*, Academic Press, New York, 1979.

[5] H. Bhadeshia: *Metal Science*, 1982, vol. 16, pp. 159–166.

[6] W. Bleck: in International Conference on TRIP-Aided High Strength Ferrous Alloys, *Using the trip effect-the dawn of a promising group of cold formable steels*, Ghent, Mainz/Aachen, 2002, pp. 13–23.

[7] T. Brambor, W. R. Clark, and M. Golder: *Political Analysis*, 2006, vol. 14, pp. 63–82.

[8] B. F. Braumoeller: *International Organization*, 2004, vol. 58, pp. 807–820.

[9] W. W. Cias: *Austenite transformation kinetics of ferrous alloys*, Climax Molybdenum Co, 1978.

[10] M. Crowder: *International Statistical Review*, 2009, vol. 77, pp. 148–149.

[11] A. A. dos Santos and R. Barbosa: *Steel Research International*, 2010, vol. 81, pp. 55–63.

[12] H.-S. Fang, J.-J. Wang, and Y.-K. Zheng: *Metallurgical and Materials Transactions A*, 1994, vol. 25, pp. 2001–2007.

[13] D. P. Foster and R. A. Stine: *Journal of the American Statistical Association*, 2004, vol. 99, pp. 303–313.

[14] M. Grossmann: *Trans. AiME*, 1942, vol. 150, pp. 6.

[15] A. F. Hayes: *Introduction to mediation, moderation, and conditional process analysis: A regression-based approach*, Guilford Publications, 2017.

[16] D. Hedeker and R. D. Gibbons: *Longitudinal data analysis*, vol. 451, John Wiley & Sons, 2006.

[17] R. R. Hocking: *Biometrics*, 1976, vol. 32, pp. 1–49.

[18] J. Kirkaldy: in Proceedings of the International Conference on Phase Transformation in Ferrous Alloys, *Prediction of microstructure and hardenability in low alloy steels*, AIME, 1983.

[19] C. Kung and J. Rayment: *Metallurgical Transactions A*, 1982, vol. 13, pp. 328–331.

[20] S. Liu, L. Yang, D. Zhu, and J. Zhang: *Metallurgical and Materials Transactions A*, 1994, vol. 25, pp. 1991–2000.

[21] S. K. Liu and J. Zhang: *Metallurgical Transactions A*, 1990, vol. 21, pp. 1517–1525.

[22] M. Maalekian: Reportnr. 1, *The effects of alloying elements on steels (I)*, Technische Universität Graz, 2007.

[23] P. Mangonon: *Metallurgical Transactions A*, 1976, vol. 7, pp. 1389–1400.

[24] H. Martin: PhD thesis, Kwame Nkrumah University of Science and Technology, Kumasi, Ghana, 2019, pp. 41–80.

[25] H. Martin, A. O. Nunoo, and A. B. C. Dadson: in 27th Biennial Conference Proceeding, Ghana Science Association *Improve the ductility of locally manufactured steel rods by tempering*, Kumasi, Ghana, 2011.

[26] J. Miettinen, S. Koskenniska, M. Somani, S. Louhenkilpi, A. Pohjonen, J. Larkiola, and J. Kömi: *Metallurgical and Materials Transactions B*, 2019, vol. 50, pp. 2853–2866.

[27] A. K. Montoya: *Behavior Research Methods*, 2019, vol. 51, pp. 61–82.

[28] K. Oi, C. Lux, and G. Purdy: *Acta Materialia*, 2000, vol. 48, pp. 2147–2155.

[29] W. Piekarska and D. Goszczyńska-Króliszewska: *Procedia Engineering*, 2016, vol. 136, pp. 82–87.

[30] W. Piekarska and M. Kubiak: *Journal of Thermal Analysis and Calorimetry*, 2012, vol. 110, pp. 159–166.

[31] A. Pohjonen, M. Somani, and D. Porter: *Metals*, 2018, vol. 8, pp. 540.

[32] A. Pohjonen, M. Somani, and D. Porter: *Computational Materials Science*, 2018, vol. 150, pp. 244–251.

[33] A. Pohjonen, M. Somani, J. Pyykkönen, J. Paananen, and D. Porter: in Key Engineering Materials, *The onset of the austenite to bainite phase transformation for different cooling paths and steel compositions*, Trans Tech Publ, 2016, vol. 716, pp. 368–375.

[34] R. Reed and H. Bhadeshia: *Materials Science and Technology*, 1992, vol. 8, pp. 421–436.

[35] *SAS/STAT software*, SAS Institute Inc., version 9.4 ed, Cary, NC, USA, 2013.

[36] N. Saunders, Z. Guo, X. Li, A. Miodownik, and J. P. Schillé: *JMatPro Software Literature*, 2004.

[37] E. Scheil: *Archiv für das Eisenhüttenwesen*, 1935, vol. 8, pp. 565–567.

[38] L. W. Sontag: *Child Development*, 1971, vol. 42, pp. 987–1002.

[39] A. Timoshenkov, P. Warczok, M. Albu, J. Klarner, E. Kozeschnik, G. Gruber, and C. Sommitsch: *Steel Research International*, 2014, vol. 85, pp. 954–967.

[40] M. T. Todinov: *Metallurgical and Materials Transactions B*, 1998, vol. 29, pp. 269–273.

[41] J. Trzaska and L. Dobrzański: *Journal of Materials Processing Technology*, 2007, vol. 192, pp. 504–510.

[42] M. Ueno and T. Inoue: *Transactions of the Iron and Steel Institute of Japan*, 1973, vol. 13, pp. 210–217.

[43] P. J. Van Der Wolk: PhD thesis, Delft: Technical University of Delft, 2001, pp. 100–200.

[44] G. F. V. Voort: *Atlas of Time-Temperature Diagrams for Irons and Steels*, ASM International, 1991.

[45] J. Wang, P. J. van der Wolk, and S. van der Zwaag: *Materials Transactions, JIM*, 2000, vol. 41, pp. 761–768.

[46] Z. S. Wieslawa Piekarska, Dorota Goszczynska: *Applied Mathematics and Computational Mechanics*, 2015, vol. 2, pp. 61–72.